Supporting Information

Mechanistic insights into the deformation and degradation of a 2D MOF

Hafeesudeen Sahabudeen[1], Qiang Zhang[1], Yue Liu[1], Matthias Heuchel[1], Rainhard Machatschek[1*]

[1]Institute of Active Polymers and Berlin-Brandenburg Center for Regenerative Therapies, Helmholtz-Zentrum Hereon, Kantstraße 55, 14513 Teltow, Germany

[*]Author to whom any correspondence should be addressed

E-mail: rainhard.machatschek@hereon.de

Materials and Methods

Materials:

5,10,15,20-tetrakis(4-carboxyphenyl)-porphyrinato palladium(II) (PdTCPP) was purchased from Porphyrin Laboratories GmbH, Scharbeutz, Germany. Co. $Cu(NO_3)_2 \cdot 3H_2O$ (99.9%) and 37 wt% hydrochloric acid (HCL) were purchased from Merck, Darmstadt, Germany. Pure grades of chloroform and methanol were purchased from Merck, Darmstadt, Germany. All chemicals were used as received without further treatment. The circular mesh TEM Grids for AFM nanoindentation measurement was purchased from Science Services GmbH, München, Germany.

Methods:

Synthesis of PdTCPP-Cu monolayer

The procedure to synthesize the PdTCPP-Cu film was adapted from the previously reported methods[1,2].
A PTFE ‘’medium area’’ Langmuir trough (Kibron, Helsinki, Finland) with a surface area of A = 280 cm^2 was filled with a $Cu(NO_3)_2.3H_2O$ (1 mM) aqueous solution as a subphase. Before filling the subphase, the trough was carefully cleaned using ethanol, acetone and water. Then, 80 µL of the 0.18 mM PdTCPP solution in chloroform/methanol solution (3:1, v/v) was spread onto the $Cu(NO_3)_2$ subphase with a microsyringe. π-MMA isotherm measurements were performed with a KSV medium area trough system by using a continuous compression speed for two barriers of 3 mm/min. The 2D array of PdTCPP-Cu at a surface pressure of 5 mN m^{-1} was transferred onto the substrate by the horizontal dipping method at room temperature. For the control experiment, 80 µL of the same PdTCPP solution was spread onto a pure water subphase. All experiments were carried out at room temperature.

Degradation of PdTCPP-Cu monolayer

Degradation experiments were carried out in a “medium area” Langmuir trough (Kibron, Helsinki, Finland) with a surface area of A = 280 cm^2. Firstly, the Langmuir trough was filled with a $Cu(NO_3)_2 \cdot 3H_2O$ (1 mM) aqueous solution as a subphase. Then, 80 µL of the 0.18 mM PdTCPP solution in chloroform/methanol solution (3:1, v/v) was spread onto the $Cu(NO_3)_2$ subphase with a microsyringe. To study the PdTCPP-Cu degradation, the monolayer was compressed and held at a surface pressure of 5 mN/m on a Milli-Q water subphase (pH = 6). After 200 min, the pH of the subphase was adjusted to 2 by injection of 5 mL of 0.3 M HCL into the subphase with V = 170 mL. All experiments were carried out at room temperature.

Interfacial Rheology

Rheology was carried out with a bicone-geometry on an MCR 502 Rheometer (Anton-Paar, Graz, Austria). The bicone had a radius of r = 25.5 mm and was immersed in a medium sized Langmuir trough. The angle of the tip of the bicone was 166.8°. The bi-conical bob disk can be rotated or oscillated and was connected to a motor, which can detect torque τ, displacement and rotational angle. The measurements were carried out under a circular slit geometry, with a custom made ring of diameter 8 cm around the bicone. The circular ring has two openings with a width of ~2 cm, which allow the film to pass into the slit between the ring and the bicone. After the Langmuir trough was filled with sub-phase of 1 mM $Cu(NO_3)_2$ or pure water, the bicone was positioned at the interface and 80 µL of PdTCPP was spread at the edge circular ring. For the oscillatory experiments, the rotational angle was oscillated with the given amplitude and frequency. A maximum shear stress τ' = 1% and frequency ν = 1 Hz were used. The interfacial shear and loss moduli were calculated using the algorithm provided with rheocompass software package. All experiments were carried out at room temperature.

Atomic Force Microscopy

Surface topography measurements and local mechanical analysis of the PdTCPP films were performed by AC-mode scanning and nanoindentation using an atomic force microscope (MFP-3D, Asylum Research, Santa Barbara, USA). AC-mode scanning was performed with OMCL-AC200TS-R3 silicon cantilevers (Olympus, Tokyo, Japan) at a scan rate of 0.5 Hz. The thickness of the PdTCPP-Cu film was determined after the film has been transferred to Si/300 nm SiO_2 substrate. A piece of mica was placed at the center of the substrate followed by horizontal transfer of PdTCPP film onto the substrate. Afterwards, the placed mica was removed, showing clear edges between the substrate and the film. The border between filled and bare substrate areas was imaged by AFM in air, and the corresponding height differences equated to the layer thickness.

The PdTCPP-Cu film was transferred on the circular TEM grid for the AFM based nanoindentation experiment. No additional treatment was carried out and the sheets adhered well to the circular holes which are important for the nanoindentation experiments. Finally, the TEM grid was fixed on a silicon chip using Kapton tape which resulted in good stability of the grid as observed by AFM imaging. Nanoindentation measurements were performed with cantilevers (OMCL-AC200-TS-R3) having a spring constant of 6.7 $N \cdot m^{-1}$.

Polarized Optical Microscopy

Polarized optical microscopy was performed at Zeiss Axio Imager A1m microscope (Carl Zeiss, Jena, Germany) equipped with crossed polarizers where a 40× magnification objective (Zeiss A-plan) was used.

Simulation methodologies

To investigate the Young's modulus of 2D MOF PdTCPP-Cu, a periodic supercell of 4x4x1 in *a*, *b*, and *c* dimensions were generated. Simulations were conducted with LAMMPS package version September 2021[3]. UFF4MOF force field[4,5] were adopted to optimize the 2D MOF to their minimum energy structure and also to reproduce Young's modulus property of PdTCPP-Cu. UFF4MOF benefits from its expansive coverage of periodic table including transition metal ions, research has also shown that it can accurately reproduce bulk modulus of varies types of MOFs[6,7,8]. No partial charges were assigned along with UFF4MOF force field, due to the introduction of partial charges could result in worse agreements with experimental observations[6,7,8]. Periodic boundary conditions applies to *x* and *y*, while *z* dimension is non-periodic and fixed to prevent the interactions between MOFs in different periodic images along *z*. To evaluate the Young's modulus, the PdTCPP-Cu 2D MOF is stretched or compressed in a selected direction, unless otherwise specified, a maximum strain ε of 4 % was considered by default. The *z* dimension is fixed, while the external pressure in the one remaining direction is kept around zero. The tensile or compression rate $\dot{\varepsilon}$ were tested and does not affect the simulation results, a value of $1x10^{-8}$/fs was used for both tensile and compression runs throughout this work. The number of atoms and the composition of MOF and water in each case are summarized in Table 1.

Table 1. Number of atoms in simulation system

	Md00	Md06	Md12	Md19	With water
$N_{atomMOF}$	1392	1396	1323	1180	1554
$N_{atomwater}$	0	0	0	0	24000

Note: Since the defect density in our simulation is defined as the number of missing building blocks divided by the number of building blocks in a perfect 2D MOF, after the deletion of building blocks (Copper paddlewheel or PdTCPP, hydrogen atoms will be added to the system, so the number of atoms in Md06 is even greater than the Md00 system. In addition, the 2D MOF in system with water is of finite size so, additional atoms were added to the cropped structure to maintain stability and ensure charge neutrality.)

Simulations were performed with time step 1 fs for initial *NVT* and *NPT* relaxations, and time step 0.5 fs were adopted for tensile and compression runs. Prior to tensile and compression runs, the atomistic models were relaxed using conjugation gradient algorithm. In addition, a self-consistent cycle was used where each cycle consisting of cell volume relaxation followed by atomic position relaxation[6]. These simulations were performed until energy difference between each cycle is less than $1x10^{-6}$ kcal/mol, or the maximum 100 iteration cycles was reached.

To calculate the Young's modulus E, uniaxial tensile and compression runs were performed in *NPT* ensemble using Nose-Hoover thermostat and barostat. The relaxation time of thermostat and barostat were 100 times and 1000 times the value of time step adopted in simulation. Van der Waals interaction cutoff distance was set to 12.5 Å, with mix arithmetic mixing rule adopted. Simulation were performed at T = 1 Kelvin, and P = 0 bar, as 1 Kelvin temperature provides kinetic energy, which allows relaxation of molecular structure under stress[9].

The Young's modulus at 1 K could be extracted from the stress–strain curve (S1)

$$\sigma_x = \varepsilon_x + C_{xx}\varepsilon_x^2 \quad \text{(S1)}$$

where E_x is Young's modulus in the selected direction, σ_x is the tensile or compression stress applied in the selected direction. ε_x is the resulting strain in the selected direction and C_{xx} is the second order elastic constant in the same direction. ε_x is the resulting deformation divided by the initial length

$$\varepsilon_x = (l_x - l_{x,0})/l_{x,0} \quad \text{(S2)}$$

Alternatively, the Young's modulus can be calculated from the second derivative of potential energy while deformation with respective to strain[9]

$$E_{pot} = k_x \times \varepsilon_x^2 + b \times \varepsilon_x \quad \text{(S3)}$$

$$E_x = 2k_x/V_0 \quad \text{(S4)}$$

As shown by (S3), E_{pot} is the potential energy of the system under deformation, k_x and b are fitting parameters of the quadratic function. V_0 is the initial volume of the 2D MOF layer, which taking into the account the layer thickness of 6 Å and initial optimized x and y dimensions. In order to make the volume calculation more accurate for 2D MOF layer with defects, the *rolling probe volume* method was used[10]. The radius of the probe was chosen so that the rolling probe volume is consistent with the volume of the perfect 2D MOF, calculated as length*width*thickness.

The Young's modulus obtained from simulations is the average of the Young's moduli E_x and E_y in x and y directions. The initial structures of the periodic 2D MOFs simulated are summarized in Fig. 4. Where the optimized unit cell of (*a*) has basal plane dimension $a = b$ = 16.65 Å, which is quite consistent with the experimental XRD value of 16.6 Å[1].

To prevent water molecules from running out of the simulation box, two reflective walls were placed on the top and bottom along the z-direction. In addition, the *openbabel* tool[11] was used to generate partial charge following the extended charge equilibration scheme[12] (EQeq) to better describe the interaction between the water and the PdTCPP-Cu monoalyer. The Young's modulus obtained at 300 K with EQeq charge is around 4 GPa which is lower than Young's modulus without a partial charge obtained at 1 K. In order to allow for sufficient relaxation of PdTCPP-Cu on water, a stepwise tensile deformation strategy was adopted. At the same time, only the PdTCPP-Cu on the water surface was stretched and kept at a certain distance each cycle. In each stepwise deformation, the PdTCPP-Cu was stretched in increments of 0.5 % of their unit cell length, and we repeated this process for 20 cycles until the 10 % maximum strain was reached. After each tensile deformation, a 20000-step relaxation of the *NVT* atomic positions was performed in LAMMPS while maintaining a specific strain on the PdTCPP-Cu along the selected direction. These were achieved by the *smd* method of LAMMPS by applying additional forces on selected groups of atoms. The well-relaxed

system, the system with PdTCPP-Cu stretched by 10 % are demonstrated in Fig. S8, and the stepwise tensile scheme and the stress-strain curve along deformation are summarized in Fig. S9 and Fig. 5b. Unlike the pure 2D MOF without water, the potential fluctuation of the MOF on the water layer is too large to extract information from it. The Young's modulus of the 2D MOF on the water layer is calculated from the slope of the stress-strain curve.

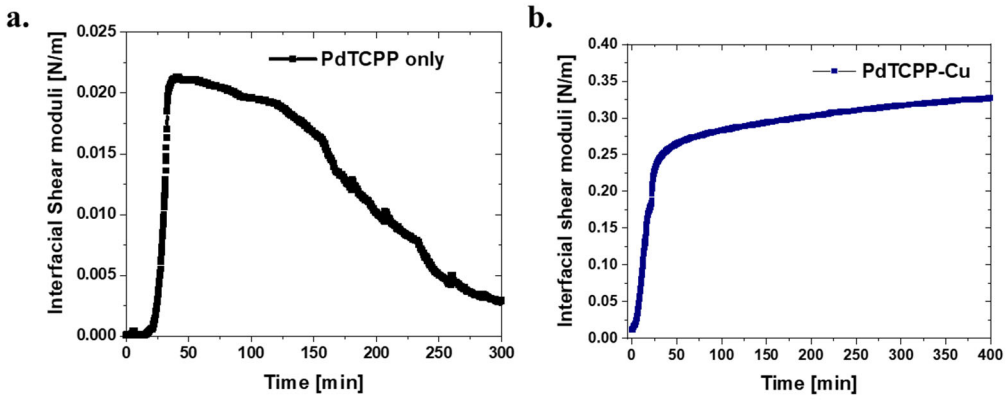

Fig. S1. Interfacial rheology of PdTCPP and PdTCPP-Cu film at the air-water interface with time sweep at a frequency of 1 Hz and Strain = 1%, a) PdTCPP monomer with water as subphase b) PdTCPP-Cu monolayers in Cu^{2+} aqueous solution.

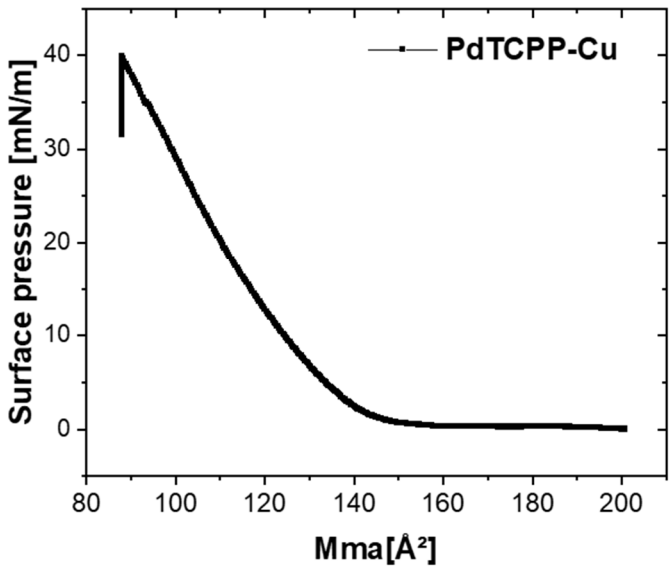

Fig. S2. Surface pressure versus molecular area (π-A) isotherm curve for PdTCPP-Cu monolayer in Cu^{2+} aqueous solution as subphase.

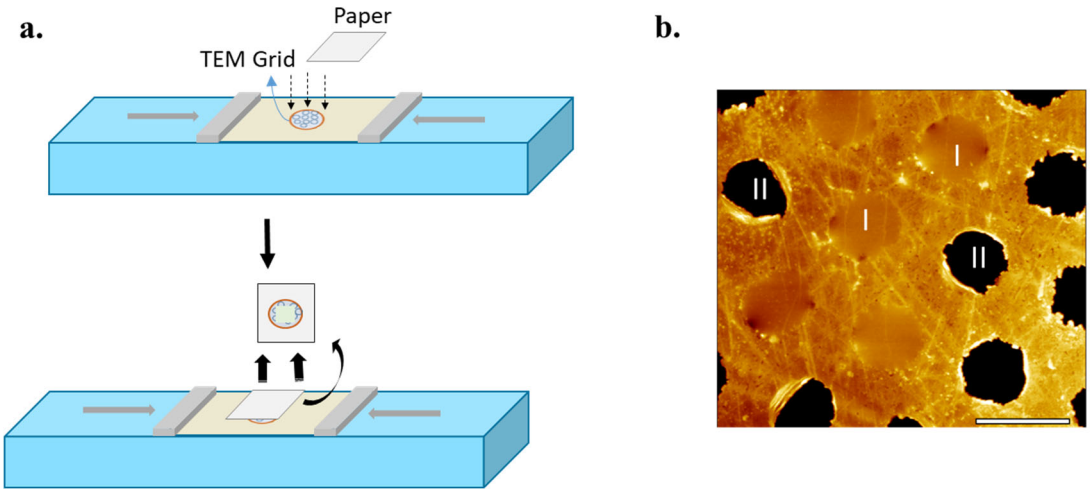

Fig. S3. Transfer method and AFM of PDTCPP-Cu monolayer on TEM grid. a) Schematic illustration for the transfer of PDTCPP-Cu monolayer onto the TEM grids. To transfer the monolayer, a TEM grid was placed at the air-water interface which is then pressed against the PdTCPP-Cu film. Then a paper was placed onto the water surface to which the TEM grids get adsorbed. The paper is slowly removed from the water surface along with the TEM grid. Subsequently, the TEM grid with a monolayer sheet can be easily isolated and used for further characterization. b) AFM image shows free-standing membranes, where the PdTCPP-Cu film was spanning an array of circular holes 7 μm in diameter, scale bar = 10 μm.

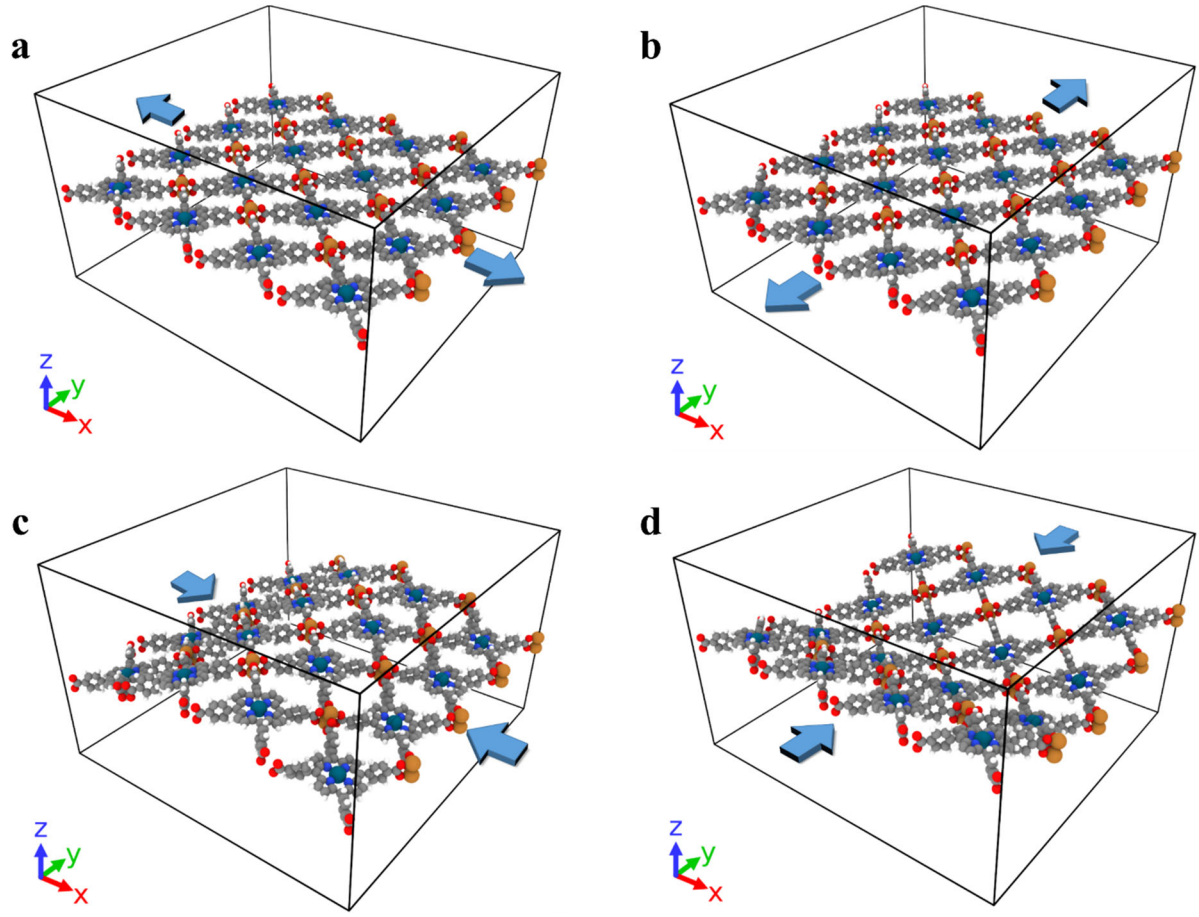

Fig. S4. PdTCPP-Cu monolayer (model Md00) under uniaxial tensile and compression mode.

Uniaxial tensile stress along a) X and b) Y direction. Uniaxial compression along c) X and d) Y direction.

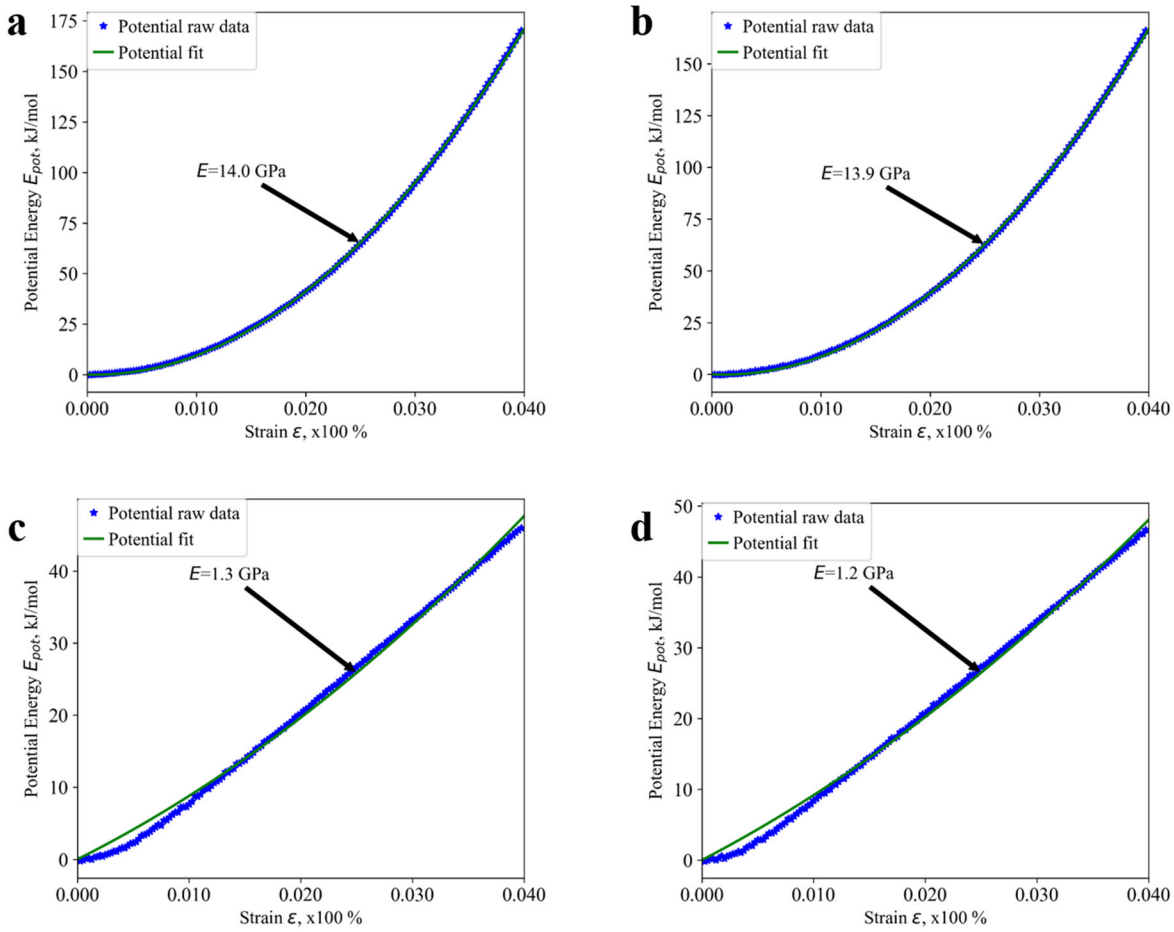

Fig. S5. Potential energy as a function of strain for perfect PdTCPP-Cu monolayer under uniaxial tensile and compression mode. Uniaxial tensile stress along a) X and b) Y direction. Uniaxial compression along c) X and d) Y direction. Fitting equation is Eqn. S3.

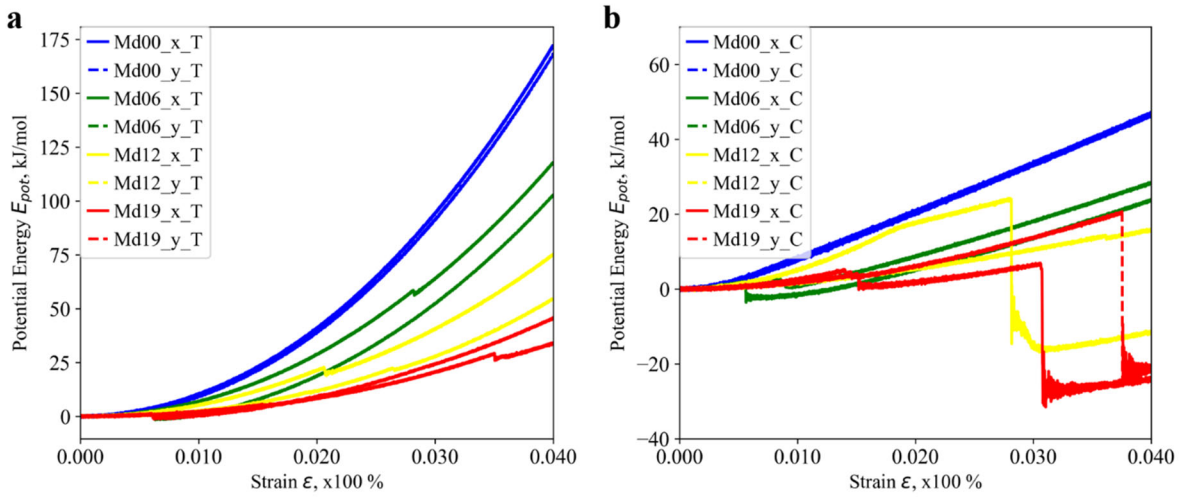

Fig. S6. Potential energy as a function of strain for PdTCPP-Cu models with different defect densities a) uniaxial tensile stress b) uniaxial tensile compression

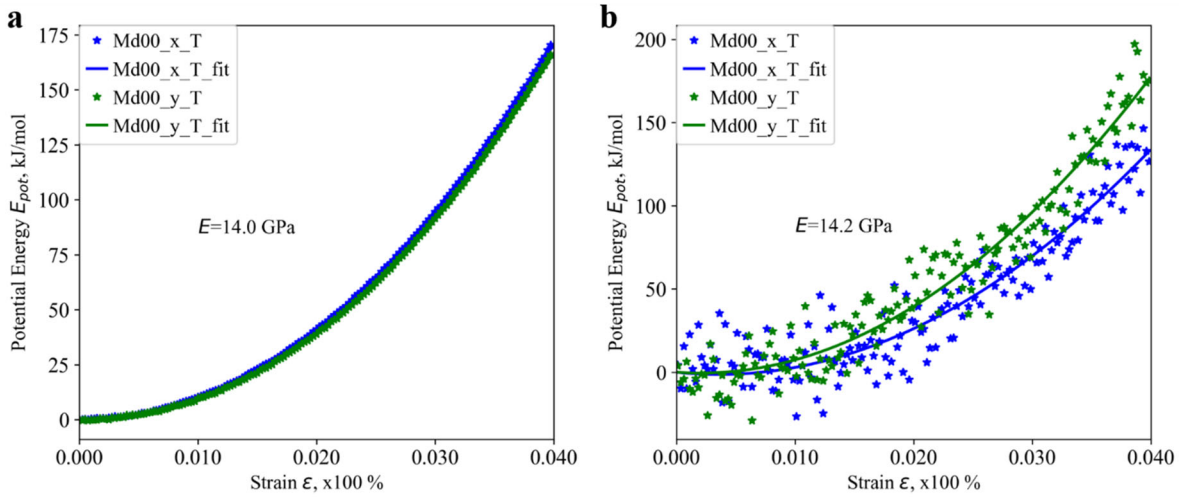

Fig. S7 Influence of temperature on Young's modulus a) Uniaxial tensile deformation at 1 K b) Uniaxial tensile deformation at 300 K.

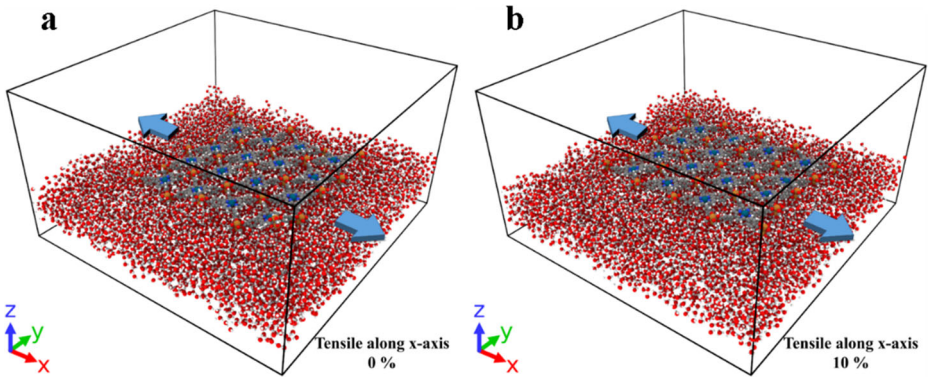

Fig. S8. PdTCPP-Cu monolayer on top of water phase at 300 K

a) without any tensile stress (b) 10 % uniaxial tensile strain.

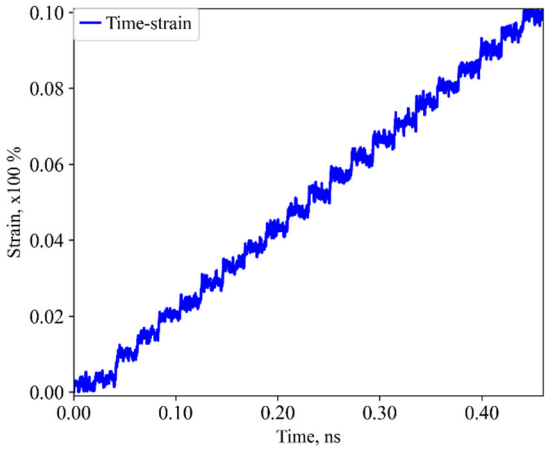

Fig. S9. Stepwise tensile deformation scheme of PdTCPP-Cu monolayer

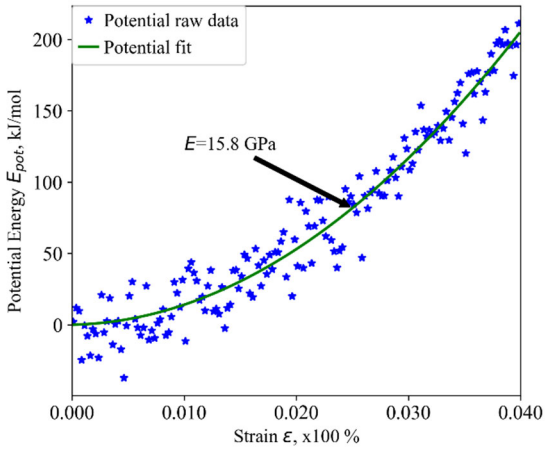

Fig. S10. Influence of partial charges on simulation results.

Potential energy as a function of strain for perfect PdTCPP-Cu monolayer under uniaxial tensile deformation along X direction without water and with EQeq charge. Fitting equation is Eqn. S3.

Reference:

(1) Makiura, R.; Konovalov, O. Interfacial Growth of Large-Area Single-Layer Metal-Organic Framework Nanosheets. *Sci Rep* **2013**, *3* (1), 2506.

(2) Motoyama, S.; Makiura, R.; Sakata, O.; Kitagawa, H. Highly Crystalline Nanofilm by Layering of Porphyrin Metal−Organic Framework Sheets. *J. Am. Chem. Soc.* **2011**, *133* (15), 5640–5643.

(3) Thompson, A. P.; Aktulga, H. M.; Berger, R.; Bolintineanu, D. S.; Brown, W. M.; Crozier, P. S.; in 't Veld, P. J.; Kohlmeyer, A.; Moore, S. G.; Nguyen, T. D.; Shan, R.; Stevens, M. J.; Tranchida, J.; Trott, C.; Plimpton, S. J. LAMMPS - a Flexible Simulation Tool for Particle-Based Materials Modeling at the Atomic, Meso, and Continuum Scales. *Computer Physics Communications* **2022**, *271*, 108171.

(4) Addicoat, M. A.; Vankova, N.; Akter, I. F.; Heine, T. Extension of the Universal Force Field to Metal–Organic Frameworks. *J. Chem. Theory Comput.* **2014**, *10* (2), 880–891.

(5) Coupry, D. E.; Addicoat, M. A.; Heine, T. Extension of the Universal Force Field for Metal–Organic Frameworks. *J. Chem. Theory Comput.* **2016**, *12* (10), 5215–5225.

(6) Boyd, P. G.; Moosavi, S. M.; Witman, M.; Smit, B. Force-Field Prediction of Materials Properties in Metal-Organic Frameworks. *J. Phys. Chem. Lett.* **2017**, *8* (2), 357–363.

(7) Madsen, R. S. K.; Stepniewska, M.; Yang, Y.; Qiao, A.; Winters, W. M. W.; Zhou, C.; König, J.; Mauro, J. C.; Yue, Y. Mixed Metal Node Effect in Zeolitic Imidazolate Frameworks. *RSC Adv.* **2022**, *12* (17), 10815–10824.

(8) Vanduyfhuys, L.; Vandenbrande, S.; Wieme, J.; Waroquier, M.; Verstraelen, T.; Van Speybroeck, V. Extension of the QuickFF Force Field Protocol for an Improved Accuracy of Structural, Vibrational, Mechanical and Thermal Properties of Metal–Organic Frameworks. *Journal of Computational Chemistry* **2018**, *39* (16), 999–1011.

(9) Li, H.; Brédas, J.-L. Impact of Structural Defects on the Elastic Properties of Two-Dimensional Covalent Organic Frameworks (2D COFs) under Tensile Stress. *Chem. Mater.* **2021**, *33* (12), 4529–4540.

(10) Voss, N. R..; Gerstein, 3V: cavity, channel and cleft volume calculator and extractor. *Nucleic Acids Res.* **2010**, *38 (web server issue)*,W555-W562.

(11) O'Boyle, N. M.; Banck, M.; James, C. M.; Morley, C.; Vandermeersch, T.; Hutchison, R. R. Open Babel: An open chemical toolbox. *J. Cheminform.* **2011**, *3*, 33

(12) Wilmer, C.E.; Kim, Q.C.; Randall, Q. S. An Extended Charge Equilibration Method. *The Journal of Phys. Chem. Let.* **2012,** *3* (17), 2506-2511